JCTC Journal of Chemical Theory and Computation

Article

pubs.acs.org/JCTC

Benchmark Study on the Triplet Excited-State Geometries and Phosphorescence Energies of Heterocyclic Compounds: Comparison Between TD-PBE0 and SAC-CI

Diane Bousquet,[†] Ryoichi Fukuda,[§,∥] Denis Jacquemin,[⊥,∇] Ilaria Ciofini,[†] Carlo Adamo,*[,†,∇] and Masahiro Ehara*[,§,∥]

[†]LECIME, Laboratoire d'Electrochimie, Chimie des Interfaces et Modélisation pour l'Energie, UMR 7575 CNRS, Ecole Nationale Supérieure de Chimie de Paris, Chimie ParisTech, 11 rue P. et M. Curie, 75231 Paris Cedex 05, France

[§]Institute for Molecular Science and Research Center for Computational Science, 38 Nishigo-naka, Myodaiji, Okazaki, 444-8585, Japan

[∥]Elements Strategy Initiative for Catalysts and Batteries (ESICB), Kyoto University, Nishikyo-ku, Kyoto 615-8520, Japan

[⊥]CEISAM, UMR CNRS 6230, BP 92208, Université de Nantes, 2 Rue de la Houssinière, 44322 Nantes, France

[∇]Institut Universitaire de France, 103 Boulevard Saint Michel, F-75005 Paris, France

Supporting Information

ABSTRACT: In this work, we investigated the properties of the triplet excited states of heterocyclic compounds including their geometries, electronic properties, and phosphorescence energies by using both the direct symmetry-adapted cluster-configuration interaction (SAC-CI) method and the TD-DFT approach with the PBE0 exchange-correlation functional (TD-PBE0). The target states are the $\pi\pi^*$ and $n\pi^*$ triplet states of furan, pyrrole, pyridine, *p*-benzoquinone, uracil, adenine, 9,10-anthraquinone, coumarin, and 1,8-naphthalimide as well as the Rydberg states. The present benchmark demonstrates that these two methods provide reasonably accurate geometries for the excited states of these heterocyclic compounds. The calculated Stokes shifts, which reflect geometry changes, were consistent for both these methods. The trends of agreement with experimental or reference values obtained for a panel of exchange-correlation functionals used to compute the absolute emission energies from the triplet states, differ from those found for the singlet excited states. Some of the low-lying triplet excited states were examined in detail for the first time, including vibrational analysis.

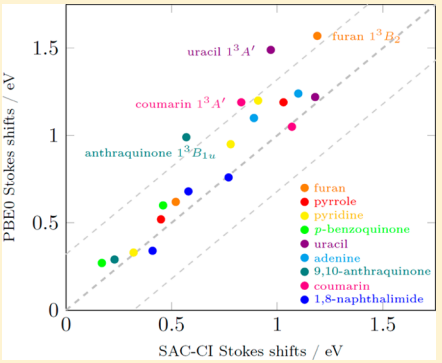

1. INTRODUCTION

Triplet excited states play an important role in chemistry, for example, in determining the magnetic properties of a material or in quenching or relaxation processes in electronically excited states. These states have attracted much attention because of their use in material technologies such as organic light-emitting diodes based on molecular phosphorescence materials,[1,2] triplet upconversion devices,[3] as well as a new-generation of solar cells with singlet fission.[4] In these molecular materials, the electronic properties and geometric structures in the triplet excited states are crucial because they determine the band structure in the emission spectra and/or excitation transfer. However, because these excited states are usually too short-lived to be observed, theoretical calculations are required to analyze their photochemistry and to design new photofunctional molecules. Thus, the development of quantum chemical methods providing reliable predictions of triplet excited state geometries and electronic properties remains of key importance.

Time-dependent density functional theory (TD-DFT) has emerged as a useful tool to analyze and predict the optical spectra of large systems. Various exchange-correlation functionals have been developed to accurately describe excited states. Numerous TD-DFT benchmarks have been performed for the vertical transitions of various types of excited states.[5−9] The TD-DFT method, relying on different functionals, has also been previously applied for the prediction of excited-state structures of linear conjugated systems[10] and, more recently, heterocyclic compounds.[11,12] It was demonstrated that global hybrid functionals such as B3LYP[13] and PBE0[14] provide similar geometries and transition energies to those obtained by using the complete active space second-order perturbation theory (CASPT2) or coupled cluster calculations that can be considered as references. However, it remains of interest to examine the TD-DFT performances of such approaches for other types of molecular systems or spin states.

Turning to ab initio wave function theories for excited states, coupled cluster approaches such as symmetry-adapted cluster/

Received: April 30, 2014
Published: June 11, 2014

   dx.doi.org/10.1021/ct5003797 | J. Chem. Theory Comput. 2014, 10, 3969−3979

Table 1. Vertical Transition Energies (ΔE, eV) Computed for Furan, Pyrrole, and Pyridine at Both TD-PBE0 and SAC-CI Levels for the Low-Lying Triplet Excited States

TD-DFT (PBE0)				SAC-CI					
D95(d,p)		6-311++G(2d,2p)		D95(d,p)		6-311G(d) Ryd.[2s2p]		expt.	
state	ΔE	state	ΔE	state	ΔE	state	ΔE	ΔE	character
				furan					
$^3B_2$	3.66	$^3B_2$	3.60	$^3B_2$	4.16	$^3B_2$	4.12	4.02[a]	$^3\pi\pi^*$
$^3A_1$	5.13	$^3A_1$	5.08	$^3A_1$	5.45	$^3A_1$	5.41	5.22[a]	$^3\pi\pi^*$
$^3A_1$	6.13	$^3A_2$	5.76	$^3A_1$	7.00	$^3A_2$	5.77		3s
$^3B_2$	7.00	$^3A_1$	6.02	$^3B_2$	7.50	$^3B_1$	6.29		$3p_y$
$^3A_2$	8.25	$^3B_1$	6.23	$^3A_2$	8.605	$^3B_2$	6.51		$3p_x$
				pyrrole					
$^3B_2$	3.99	$^3B_2$	3.96	$^3B_2$	4.43	$^3B_2$	4.41	4.21[a]	$^3\pi\pi^*$
$^3A_1$	5.21	$^3A_2$	4.97	$^3A_1$	5.49	$^3A_2$	4.94		3s
$^3A_1$	5.76	$^3A_1$	5.16	$^3A_1$	6.50	$^3A_1$	5.44	5.10[a]	$^3\pi\pi^*$
$^3B_2$	6.34	$^3A_1$	5.64	$^3B_2$	6.78	$^3B_1$	5.60		$3p_y$
$^3A_2$	7.11	$^3B_1$	5.69	$^3A_2$	7.59	$^3A_2$	5.67		$3p_z$
				pyridine					
$^3A_1$	3.68	$^3A_1$	3.68	$^3A_1$	4.10	$^3A_1$	4.12	~4.1[b]	$^3\pi\pi^*$
$^3B_1$	4.41	$^3B_1$	4.07	$^3B_1$	4.50	$^3B_1$	4.46		$^3n\pi^*$
$^3B_2$	4.51	$^3B_2$	4.43	$^3B_2$	4.86	$^3B_2$	4.79	~4.84[b]	$^3\pi\pi^*$
$^3A_1$	4.84	$^3A_1$	4.80	$^3A_1$	5.11	$^3A_1$	5.08		$^3\pi\pi^*$
$^3A_2$	5.01	$^3A_2$	5.04	$^3A_2$	5.44	$^3A_2$	5.44	~5.4[b]	$^3n\pi^*$

[a]Ref 41. [b]Refs 42−44.

configuration interaction (SAC-CI),[15,16] coupled cluster linear response theory (CC-LRT),[17,18] and equation-of-motion coupled cluster (EOM-CC)[19,20] have all been recognized as reliable tools. Analytical derivatives have also been implemented for these methods, which facilitates the determination of excited-state properties beyond transition energies, including geometries, vibrational frequencies, and relaxation energies. However, it is still challenging to investigate these characteristics for systems that require large-scale calculations due to the unfavorable computational scaling of these methods.

The SAC-CI method has been applied to various molecular excited states, including higher spin-multiplicity systems such as triplet excited states,[21,22] and the analytical energy gradients of the method (first derivatives) have also been formulated and implemented for various spin multiplicities.[23−26] The method has been used to calculate the equilibrium geometries and one-electron properties of electronic states,[27] and a direct algorithm of the SAC/SAC-CI method (direct SAC-CI) has been developed to enable efficient yet accurate calculations.[28] We have performed a systematic examination of excitation operators and established a useful criteria for the perturbation selection, allowing the reliable calculation of excited-state geometries of large systems.

Recently, we have systematically investigated the excited state geometries of some π-conjugated heterocyclic compounds in their singlet excited states.[11] For these compounds, the global hybrid functionals PBE0 and B3LYP provided better results than other functionals with respect to both structures and energies of fluorescent states, with mean deviations of emission energies computed to be 0.2 (PBE0) and 0.3 eV (B3LYP). On the other hand, obtaining descriptions of the electronic triplet states with TD-DFT still implies some difficulties.[29,30] A systematic TD-DFT examination using 34 DFT functionals showed that the trends (relative accuracies of the different functionals) obtained for singlet excited states do not necessarily hold for triplet excited states, for example, BMK and M06-2X functionals perform better in the prediction of singlet−triplet transition energies, which contrasts with singlets.[9] The triplet states of similar system were also studied by TD-DFT (PBE0) and the second-order approximated coupled-cluster with the resolution of identity (RICC2).[31] Recently, triplet instability in the TD-DFT approach was pointed out,[32] confirming that the calculation of triplet energies with TD-DFT generally implies significantly larger errors than the corresponding singlet energies. The long-range corrected functionals suffer from the instability in the ground state originated in the large amount of Hartee-Fock exchange.[33] This motivated us to examine the various DFT functionals for calculating the geometry in the triplet excited states, within the framework of TD-DFT. Indeed, detailed analysis of triplet excited state geometry is, to the best of our knowledge, missing.

In this work, we systematically investigated the geometries of low-lying valence triplet excited states of nine π-conjugated heterocyclic compounds that were used in a previous work[11] to assess singlet excited states. The compounds studied are furan, pyrrole, pyridine, *p*-benzoquinone, uracil, adenine, 9,10-anthraquinone, coumarin, and 1,8-naphthalimide. The direct SAC-CI and TD-PBE0 methods were compared with respect to both triplet excited state geometry and phosphorescent-state energy. The target states were not limited to the lowest excited state: some higher excited states have also been examined. The results of the two approaches were compared in detail and the characteristics of the methods discussed.

2. COMPUTATIONAL DETAILS

All ab initio and DFT calculations, namely, direct SAC-CI and TD-DFT calculations with PBE0[14] and other functionals (reported and discussed in section 3.3) were performed with Gaussian 09 revision B01.[34] The vertical singlet-to-triplet transition energies were calculated by using the optimized ground-state geometries to examine the nature of the low-lying

Table 2. Vertical Transition Energies (ΔE, eV) Computed for *p*-Benzoquinone, Uracil, and Adenine at Both TD-PBE0 and SAC-CI Levels for the Low-Lying Triplet Excited States

TD-DFT (PBE0)				SAC-CI				
D95(d,p)		6-311++G(2d,2p)		D95(d,p)		expt.		other theory
state	ΔE	state	ΔE	state	ΔE	ΔE	character	ΔE
				p-benzoquinone				
$^3B_{1g}$	2.00	$^3B_{1g}$	2.01	$^3B_{1g}$	2.58	2.28[a], 2.31[b]	$^3n_g^--\pi_g^-*$	2.17[d]
^3A_u	2.21	^3A_u	2.23	^3A_u	2.75	2.32[a], 2.35[b], 2.29[c]	$^3n_u^+-\pi_g^-*$	2.27[d]
$^3B_{1u}$	2.24	$^3B_{1u}$	2.28	$^3B_{1u}$	3.04		$^3\pi_u^+-\pi_g^-*$	2.91[d]
$^3B_{3g}$	2.69	$^3B_{3g}$	2.66	$^3B_{3g}$	3.44		$^3\pi_g^+-\pi_g^-*$	3.19[d]
$^3B_{1u}$	4.81	$^3B_{1u}$	4.79	^3A_g	5.54		$^3\pi_g^+-\pi_u^-*$	
				uracil				
$^3A'$	3.37	$^3A'$	3.35	$^3A'$	3.67	3.60 ± 0.08[e], 3.35 ± 0.08[f]	$^3\pi\pi*$	3.62[g], 3.86[h], 3.80[i]
$^3A''$	4.36	$^3A''$	4.36	$^3A''$	4.59		$^3n\pi*$	4.98[h], 4.71[i]
$^3A'$	4.80	$^3A'$	4.77	$^3A'$	5.39		$^3\pi\pi*$	
$^3A'$	5.55	$^3A'$	5.46	$^3A''$	6.10		$^3n\pi*$	
$^3A''$	5.69	$^3A''$	5.66	$^3A'$	6.12		$^3\pi\pi*$	
				adenine				
$^3A'$	3.51	$^3A'$	3.48	$^3A'$	3.81		$^3\pi\pi*$	3.71[g]
$^3A'$	4.54	$^3A'$	4.47	$^3A'$	4.84		$^3\pi\pi*$	
$^3A''$	4.80	$^3A''$	4.77	$^3A''$	4.98		$^3n\pi*$	
$^3A'$	4.84	$^3A'$	4.81	$^3A'$	5.32		$^3\pi\pi*$	
$^3A'$	5.20	$^3A'$	5.18	$^3A''$	5.50		$^3n\pi*$	

[a]Ref 51. [b]Refs 50 and 52. [c]Ref 49. [d]CASPT2 in ref 56. [e]Ref 53 (thymine). [f]Ref 53 (bromouracil). [g]B3LYP in ref 54. [h]EOM-CC in ref 58. [i]CASPT2 in ref 56.

excited states. The ground-state geometries were taken from our previous work and were based on SAC/D95(d,p) optimizations.[11] The TD-PBE0 calculations of the vertical transition energies were done using the double-ζ plus polarization basis sets of Dunning, D95(d,p),[35] the Pople triple-ζ plus double polarization and diffuse functions, 6-311++G(2d,2p),[36] and the aug-cc-pVTZ[37] atomic basis sets. The geometry optimization by TD-PBE0 was performed with the D95(d) basis set. The emission (phosphorescence) energy was calculated as vertical transition from the equilibrium structure of the triplet state.

In the SAC-CI calculations for the vertical transitions and geometry optimizations, the double-ζ basis sets D95(d,p) and D95(d) were used, respectively. For the vertical absorption of furan, pyrrole, and pyridine, we also adopted basis sets with diffuse functions, namely, 6-311G(d) plus two sets of Rydberg *s* and *p* functions [2s2p] to accurately describe the low-lying Rydberg states. The exponents of these Rydberg functions [2s2p] were obtained by multiplying the original Dunning Rydberg functions by factors 1.9 and 0.85.[38] The level-three accuracy (energy thresholds of $\lambda_g = 10^{-6}$ au and $\lambda_e = 10^{-7}$ au) was adopted for the perturbation selection.[39] All the product S_2S_2, R_1S_2 and R_2S_2 terms were included without selecting operators as in the usual procedure of direct SAC-CI;[28] R_n and S_n represent the excitation operators for the ground and exited states, where the subscript *n* denotes the excitation level. In the geometry optimizations, macroiteration[40] was done three times and the structures were converged, with the CIS/D95(d) derived geometry being used as initial geometry. For uracil and adenine, although the C_s structure is not a local minimum in the ground state, this symmetry was imposed for both ground and excited states to avoid a conical intersection.

3. RESULTS AND DISCUSSION

3.1. Vertical Transition Energy. The vertical transition (S_0 to T_n) energies of the low-lying triplet exited states of the studied molecules were calculated to determine the nature of the excited states as well as to compare the different methodologies using a constant ground state geometry. Indeed, these calculations enable the analysis of the methodological errors that arise when calculating separately the electronic state and the stable geometry, in contrast to emission (phosphorescence) where structural and energetic effects are mixed. The calculated vertical transition energies of five low-lying triplet excited states of furan, pyrrole, and pyridine are summarized in Table 1 together with the corresponding experimental values.[41−44] The TD-PBE0 values obtained with *aug*-cc-pVTZ are given in the Supporting Information (SI). Because these molecules also present Rydberg states in the low-energy region, two types of basis sets were needed: D95(d,p), which is accurate for valence excited states only, and 6-311++G(2d,2p), which can describe both valence and Rydberg excited states.

For furan and pyrrole, the two lowest-lying states $^3B_2$ and $^3A_1$, which are characterized as valence excited states, correspond to $\pi\pi*$ transitions.[45] For these states, TD-PBE0 provided transition energies smaller than their SAC-CI counterparts by 0.3−0.5 eV, whereas the experimental values are bracketed by these two theoretical values. For instance, the theoretical values for furan are 3.66 and 5.13 eV (TD-PBE0), and 4.12 and 5.41 eV (SAC-CI) for the $^3B_2$ and $^3A_1$ states, respectively, whereas experimental values of 4.02 and 5.22 eV were observed with electron energy loss (EEL) spectroscopy.[41] The singlet $^1B_2$ state is located around 2 eV above, indicating a large exchange interaction for this state. The results obtained at the PBE0/6-311G++(2d,2p) level indicate that the transition energies are converged to 0.1 eV. Considering the slower convergence of the ab initio method with respect to the basis

set, the differences between TD-PBE0 and SAC-CI values are nevertheless slightly dependent on the basis set. The other three higher states, $^3A_2$, $^3B_1$, and $^3B_2$ require the inclusion of diffuse orbitals, and correlate to 3s, $3p_y$, and $3p_x$ Rydberg states, respectively. The singlet−triplet splitting values for these three Rydberg states were calculated to be approximately 0.2 eV.

For pyridine, among the first five computed states, three are optically forbidden and the corresponding experimental singlet−triplet transitions are clearly identified at 4.10, 4.84, and 5.43 eV.[42−44] The SAC-CI/6-311G(d) Ryd.[2s2p] method provides very accurate results, with the transition energies to $^3A_1$, $^3B_2$, and $^3A_2$ states of 4.12, 4.79, and 5.44 eV, respectively. The CASPT2[46] and MRDCI[42] calculations gave slightly lower transition energies for these states, but they were in reasonable agreement with the present data, as well as with TD-PBE0 results. The remaining two transitions were computed by SAC-CI to have energies of 4.46 and 5.08 eV, which overlap with the singlet excited states observed at 4.44 and 4.99 eV,[42,47] respectively, and are therefore difficult to observe experimentally. These states are characterized as $n\pi^*$ or $\pi\pi^*$ transitions. As can be seen in Table 1, TD-PBE0 and SAC-CI calculations provide relatively similar transition energies, but for a significantly smaller energy of the first triplet state with PBE0 (−0.44 eV compared to SAC-CI). In contrast with the singlet excited states, the basis set dependence of the SAC-CI result is small for the triplet states, and SAC-CI calculations with an even flexible basis set provided similar results.[48]

The vertical transition energies (ΔE, eV) computed for biologically important molecules *p*-benzoquinone, uracil, and adenine, are collected together with experimental values in Table 2.[49−53] Because of their practical significance, the excited states of these molecules have been intensively studied in many theoretical works by using methods such as DFT,[54] CASPT2,[55,56] SAC-CI,[57] and EOM-CC.[58] Here, we therefore focus on the low-lying triplet excited states.

For *p*-benzoquinone, the lowest triplet valence excited states have been investigated in detail in experimental[51,52] and theoretical[55] works. After some controversial discussions, it was shown that the CASPT2 assignments were consistent with the experimental observations, and the order of the triplet excited states was established to be $1^3B_{1g} < 1^3A_u < 1^3B_{1u} < 1^3B_{3g}$.[55] In the calculations presented here, these four low-lying triplet valence excited states were obtained in the same order, the TD-PBE0 and SAC-CI values again bracketing the measured data. These states are characterized as the transitions from n_g^- and n_u^+ orbitals to $\pi_g^-{}^*$ orbital (1^3B_{1g} and 1^3A_u) and from the π_u^+ and π_g^+ orbitals to the $\pi_g^-{}^*$ orbital (1^3B_{1u} and 1^3B_{3g}). The agreement between the transition energies calculated by TD-PBE0 and SAC-CI is acceptable for the first two states, but worse for the $\pi\pi^*$ transition, which was also observed in the case of singlet excitations. Compared with the calculated CASPT2 values,[55] TD-PBE0 gave better agreement for $n\pi^*$ transitions and the SAC-CI values were closer for the $\pi\pi^*$ transitions.

A systematic theoretical study on the singlet−triplet gap of nucleobases using B3LYP and CCSD(T) calculations has been undertaken previously,[54] while Abouaf et al.[53] reported the results of electron impact spectroscopy for the lowest triplet states of bromouracil and thymine. For the $T_1(1^3A')$ state, TD-PBE0 and SAC-CI calculations gave vertical transition energies of 3.37 and 3.67 eV, respectively, compared with the experimentally determined value of 3.60 ± 0.08 eV (obtained for thymine).[53] The values calculated by TD-PBE0 and SAC-CI are also consistent with their B3LYP counterpart (3.62 eV).[54] The agreement between TD-PBE0 and SAC-CI remains reasonable for the higher triplet excited states of this molecule. For example, the energy of the second triplet state, that is, the $1^3A''$ state, was computed to be 4.36 and 4.59 eV by using TD-PBE0 and SAC-CI, respectively. To our knowledge, no accurate experimental reference is available for adenine, and the reference theoretical value of 3.71 eV was obtained at the B3LYP/6-311++G(3df,2p) level of theory (not TD-DFT). The present TD-PBE0 and SAC-CI calculations provided similar values of 3.51 and 3.81 eV, respectively, for the $1^3A'$ state. The sequence of the low-lying triplet states for both nucleobases is slightly different with both methods.

The results obtained by applying the SAC-CI and TD-PBE0 calculations for three representative fluorophores, 9,10-anthraquinone, coumarin, and 1,8-naphthalimide, are summarized in Table 3 with experimental values.[49,59] Although the photophysical properties of these dyes and their derivatives (i.e., absorption or fluorescence) have been investigated in detail with respect to solvatochromism,[30] fewer studies on their triplet excited states are available. In the present work, the five low-lying triplet excited states of these molecules are examined. Since these are low-lying excited valence states, calculations with the D95(d) basis set should be sufficient to correctly describe the essential character of the states.

Table 3. Vertical Transition Energies (ΔE, eV) Computed for 9,10-Anthraquinone, Coumarin, and 1,8-Naphthalimide at Both TD-PBE0 and SAC-CI Levels for the Low-Lying Triplet Excited States

TD-DFT (PBE0)				SAC-CI			
D95(d,p)		6-311+ +G(2d,2p)		D95(d,p)			
state	ΔE	state	ΔE	state	ΔE	expt.	character
9,10-anthraquinone							
$^3B_{1g}$	2.57	$^3B_{1g}$	2.56	$^3B_{1g}$	2.74	2.73[a]	$^3n\pi^*$
$^3B_{1u}$	2.79	$^3B_{1u}$	2.80	^3A_u	2.99		$^3n\pi^*$
^3A_u	2.82	^3A_u	2.82	$^3B_{1u}$	3.48		$^3\pi\pi^*$
$^3B_{3g}$	2.95	$^3B_{3g}$	2.92	$^3B_{3g}$	3.64		$^3\pi\pi^*$
^3A_g	3.17	^3A_g	3.14	^3A_g	3.88		$^3\pi\pi^*$
coumarin							
$^3A'$	2.73	$^3A'$	2.73	$^3A'$	3.09	2.73[b]	$^3\pi\pi^*$
$^3A'$	3.58	$^3A'$	3.57	$^3A'$	4.00		$^3\pi\pi^*$
$^3A'$	4.02	$^3A'$	3.99	$^3A''$	4.40		$^3n\pi^*$
$^3A''$	4.19	$^3A''$	4.21	$^3A'$	4.43		$^3\pi\pi^*$
$^3A'$	4.57	$^3A'$	4.52	$^3A''$	6.44		$^3n\pi^*$
1,8-naphthalimide							
$^3A_1$	2.28	$^3A_1$	2.26	$^3A_1$	2.60		$^3\pi\pi^*$
$^3B_2$	3.42	$^3B_2$	3.39	$^3B_1$	3.83		$^3n\pi^*$
$^3B_1$	3.59	$^3B_1$	3.59	$^3B_2$	3.99		$^3\pi\pi^*$
$^3B_2$	3.75	$^3B_2$	3.72	$^3A_2$	4.31		$^3n\pi^*$
$^3B_2$	4.05	$^3B_2$	4.05				

[a]Ref 49. [b]Ref 59.

Among the five triplet states of 9,10-anthraquinone, 1^3B_{1g} and 1^3A_u states are located in the low-energy region, similar to the corresponding singlet excited states, whereas the 1^3B_{1u} state is very stable compared to the corresponding singlet state; the calculated SAC-CI transition energies are 2.74, 2.99, and 3.48 eV for 1^3B_{1g}, 1^3A_u, and 1^3B_{1u}, respectively, whereas the singlet states appear at 3.12, 3.36, and 5.30 eV, respectively. Although

the results obtained by both methods are in reasonable agreement, the order of the 1^3A_u and 1^3B_{1u} states is reversed when going from TD-PBE0 to SAC-CI. For coumarin, the lowest $\pi\pi^*$ and $n\pi^*$ states are found at 3.09 and 4.40 eV (SAC-CI) and at 2.73 and 4.19 eV (TD-PBE0), respectively. To our knowledge, there are no previous ab initio or DFT results available for the triplet states of this molecule. For 1,8-naphthalimide, the 1^3A_1 and 1^3B_2 states, which are characterized as $\pi\pi^*$ transitions, are computed to be 2.28 and 3.42 eV (TD-PBE0), and 2.60 and 3.99 eV (SAC-CI), respectively. The other low-lying states, 1^3B_1 and 1^3A_2, are ascribed as $n\pi^*$ transitions.

Overall, we can therefore conclude that for most cases, TD-PBE0 and SAC-CI provide the same ordering for the triplet states, the transition energies obtained with the former method being almost systematically smaller than with the latter approach, the typical deviations being of ca. 0.3−0.5 eV for the lowest-lying states. At this stage, it is difficult to ascribe these deviations as a TD-DFT error, as the available experimental data (or those obtained with highly accurate theoretical schemes, e.g., CAS-PT2) are often bracketed by TD-PBE0 (lower) and SAC-CI (higher) results. Eventually, we underline that a more detailed analysis on the basis set dependence for TD-PBE0 calculations, as well as a study of functional dependence can be found in section 3.3 and in the SI, but do not change these trends.

3.2. Excited-State Structure and Emission Energy. Geometry optimizations of the low-lying triplet excited states of all nine molecules were performed at the SAC-CI and TD-PBE0 levels using the D95(d) basis set. Unlike singlet excited states, the valence triplet excited states are located below the Rydberg states even for small molecules such as furan and pyrrole, and therefore, all the states could be optimized by using the D95(d) basis set. Consequently, the standard optimization procedure for SAC-CI can be used, although it presents difficulties for optimization of the Rydberg states. The molecular structures and the definition of the atomic numbering are given in Figure 1. The geometry relaxation in the triplet excited states, namely, the bond-length changes of the backbone structure are displayed in Figures 2−4. These values are also compared with the results of our previous study on the singlet excited states.[11] The vertical emission (phosphorescence) energy and the difference in the optimized geometries (root-mean-square deviation, rmsd) obtained by using the two methods are summarized in Table 4. The detailed comparison of the calculated geometrical parameters can be found in SI. The functional dependence regarding emission energies and structural parameters are discussed in section 3.3. Cartesian coordinates of all systems are given in the SI.

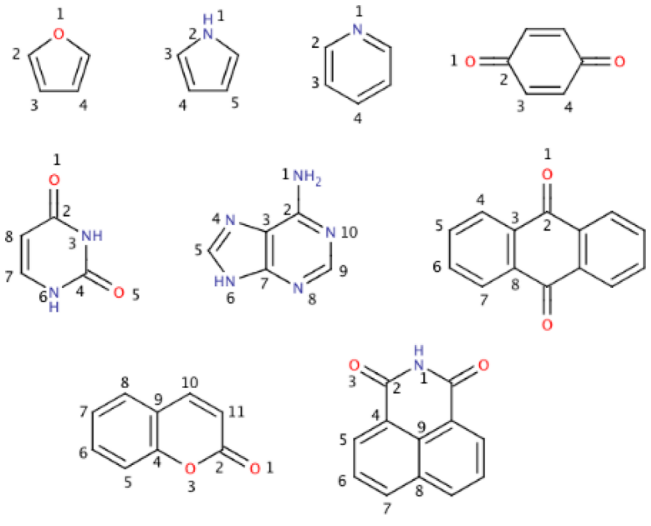

Figure 1. Molecular structures and atom numbering of the heterocyclic compounds studied in the present work. The numbering of atoms is different from that used in IUPAC.

The geometries of the singlet excited states of furan, pyrrole, and pyridine have been intensively investigated and structures with lower point group symmetry have been found to be local minima.[60−62] Here, we carried out vibrational analysis by performing CIS/D95(d) calculations for all triplet excited states and found that the C_{2v} structures are saddle points, as shown in the SI. The calculated geometrical changes of the low-lying triplet excited states of these three molecules are summarized in Figure 2.

For furan, we nevertheless perform TD-PBE0 and SAC-CI calculations using the C_{2v} point group, but the true C_1 minimum was also located with SAC-CI. As seen in Figure 2, both the geometrical changes and bond alternations are larger in the 1^3B_2 state than in the corresponding singlet excited state. In the second triplet state (1^3A_1), the C_3-C_4 bond is much more elongated than in the singlet 1^1A_1 state, whereas the change with respect to the ground state geometry of the C_2-C_3 bond is smaller. In all cases, the geometrical changes provided by TD-PBE0 and SAC-CI are similar. The rmsd of backbone bond lengths computed by comparing the two methods are 0.014 and 0.008 Å for the 1^3B_2 and 1^3A_1 states, respectively, and 0.003 and 0.011 Å for the singlet states, taking the ground-state as reference.[11] In contrast, the deviations of the emission energies between the two methods are found to be large and significantly exceeding those obtained for the fluorescence energies. As stated in the introduction, it was reported that the emission energies can be estimated with much smaller errors by using BMK or M06-2X functionals.[9]

The geometry changes of the valence triplet 1^3B_2 and 1^3A_1 states of pyrrole are similar to those of furan (Figure 2). The agreement between the equilibrium bond lengths optimized by SAC-CI and TD-PBE0 was satisfactory, and the average variations are alike to those observed for the singlet excited states, with rmsd values of 0.009 and 0.003 Å for 1^3B_2 and 1^3A_1 states, respectively, compared with 0.006 and 0.009 Å for the singlet states.[11] In 1^3A_1, all bond lengths were elongated with respect to the ground state geometry, and some variations differ from those in singlet excited state; for example, the C_4-C_5 bond length is larger (smaller) than the C_3-C_4 bond in 1^3A_1 (1^1A_1). The deviations in emission energies between SAC-CI and TD-PBE0 are 0.60 and 0.35 eV, respectively, with the former giving lower transition energies than the latter, as observed for the absorption (see previous section).

For pyridine, the optimization was done for three C_{2v} structures (1^3A_1, 1^3B_1, and 1^3B_2 states) and one C_s structure (1A′ state). Among these, the 1^3B_1, 1^3B_2, and 1A′ states were confirmed to be minima by the vibrational analysis. Because the 1^1A_1 state is much higher in energy, we compare the lowest singlet and triplet states ($^1B_1$ and $^3A_1$; Figure 2). A characteristic change in the geometry was obtained in the 1^3A_1 state, with a significant difference for the C_2-C_3 bond, which is elongated (Δr > ∼0.1 Å). The agreement between the geometries obtained by PBE0 and SAC-CI is satisfactory, with rmsd values between 0.003 and 0.009 Å for these three structures, whereas

dx.doi.org/10.1021/ct5003797 | J. Chem. Theory Comput. 2014, 10, 3969−3979

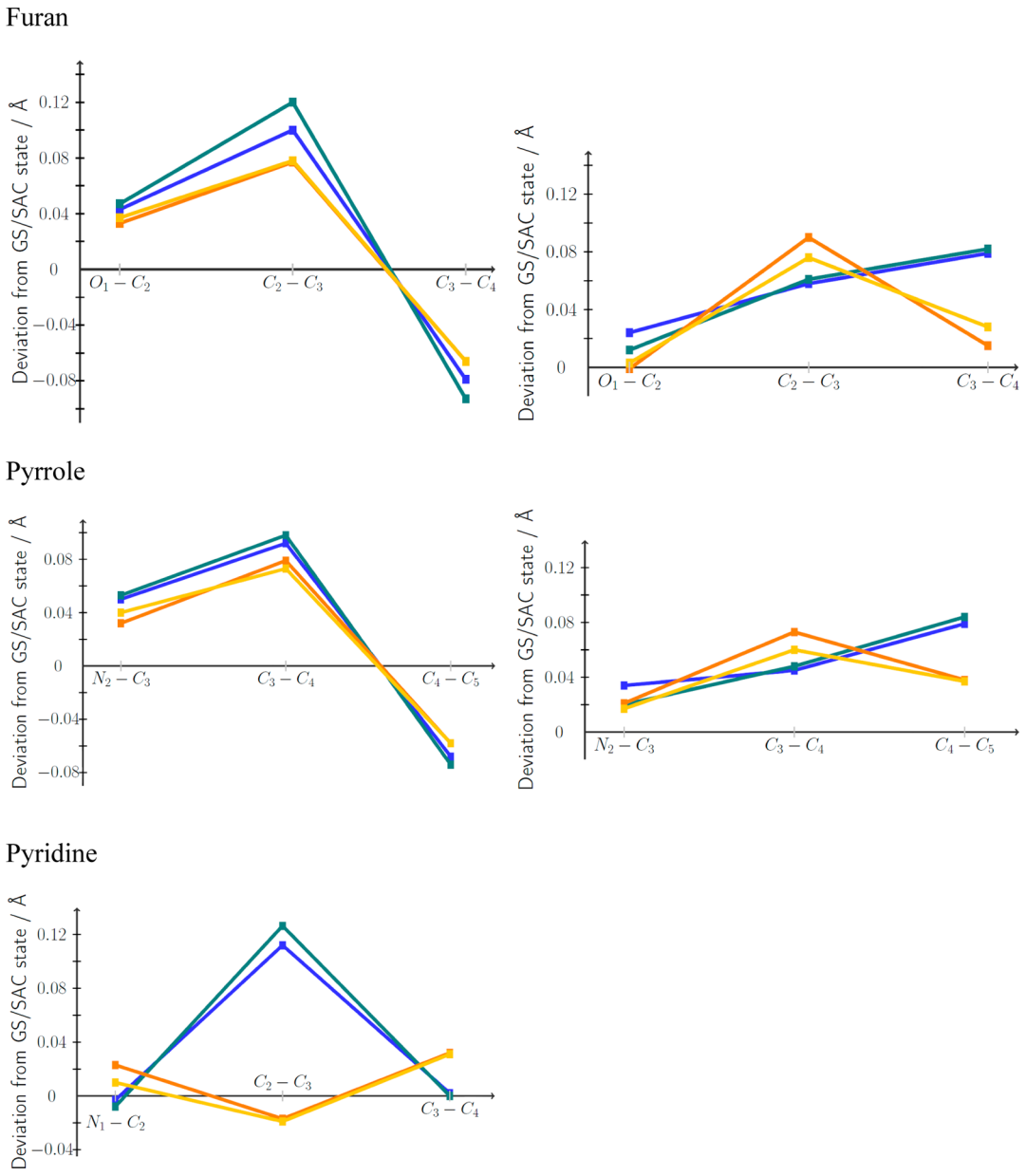

Figure 2. Geometry changes relative to the ground state for the singlet[11] and triplet excited states of furan (left, $^{1,3}B_2$; right, $^{1,3}A_1$), pyrrole (left, $^{1,3}B_2$; right, $^{1,3}A_1$), and pyridine ($^1B_1$, $^3A_1$) calculated by SAC-CI (singlet, orange; triplet, blue) and TD-PBE0 (singlet, yellow; triplet, green).

the TD-PBE0 emission energies are lower by 0.36−0.49 eV than the corresponding SAC-CI values.

The geometry changes of the lowest triplet state for *p*-benzoquinone, uracil, and adenine are compared in Figure 3. The optimized parameters for higher states are collected in the SI. The true minima are nonplanar structures for uracil and adenine, as noted in section 2. The vibrational frequency analysis was done for the low-lying excited states of these molecules and the results can be found in the SI. For the excited states of uracil and adenine, the C_s structures were also found to be saddle points and the same hold for the ground state as well: the structures of these molecules were calculated in a C_s restricted structure to avoid conical intersection.

For *p*-benzoquinone, five low-lying triplet excited states (all D_{2h} symmetry) and one lowest C_{2v} structure were optimized by SAC-CI as summarized in the SI. Among these states, the 1^3B_{3g}, 1^3A_u, 1^3A_g, and 1^3B_2 states were found to be local minima based on vibrational analysis (SI). The equilibrium structures of all these low-lying excited states, but for the 1^3A_g state, were calculated. With SAC-CI, the emission energies for the 1^3A_u and 1^3B_{1g} states were found at 2.29 and 2.41 eV, respectively, which is in good agreement with the recent experimental values of 2.28 and 2.31 eV,[63] respectively. Focusing on these 1^3A_u and 1^3B_{1g} states, a bond elongation occurs in the O_1−C_2 and C_3−C_4 bonds, whereas a contraction occurs for C_2−C_3. Although the rmsd values for the calculated bond lengths are smaller (0.01 Å, Table 4), the emission energies computed at the TD-PBE0 level were significantly underestimated and this parallels the vertical transition energy computed previously.

For uracil, C_s−constrained structures of the $1^3A'$ and $1^3A''$ states have been obtained. The changes in geometry from the ground state computed for the $1^3A'$ state are given in Figure 3 and only the C_7—C_8 bond undergoes significant changes, all other bonds varying by less than ca. 0.02 Å. In fact, the bond

dx.doi.org/10.1021/ct5003797 | J. Chem. Theory Comput. 2014, 10, 3969−3979

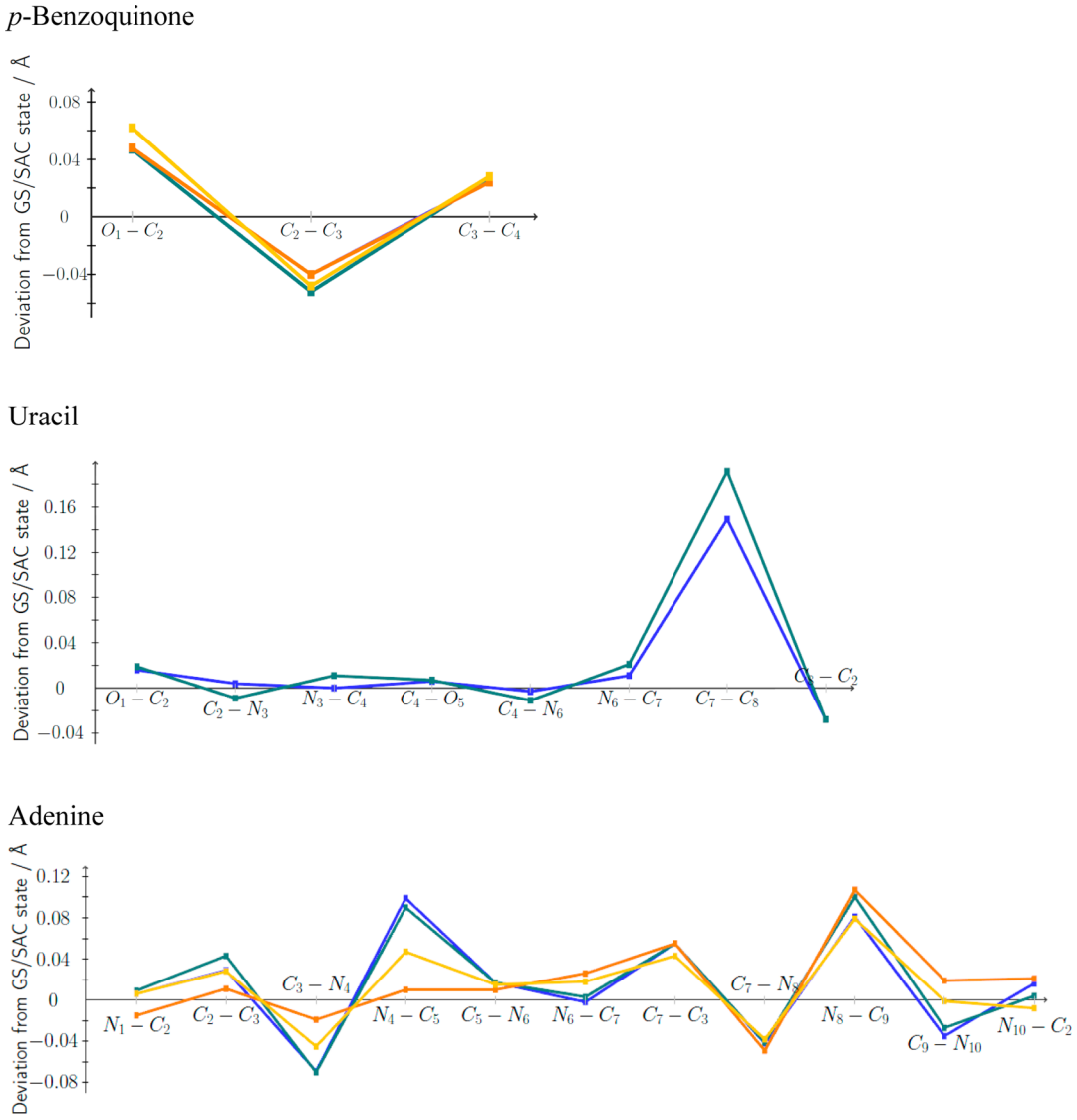

Figure 3. Geometry changes relative to the ground state for the singlet[11] and triplet excited states of *p*-benzoquinone ($^{1,3}A_u$), uracil ($^3A'$), and adenine ($^{1,3}A'$) calculated by SAC-CI (singlet: orange, triplet: blue) and TD-PBE0 (singlet: yellow, triplet: green).

alternation change is localized in the $C_7{=}C_8{-}C_2{=}O_1$ unit. The rmsd values of the bond lengths in uracil calculated by TD-PBE0 and SAC-CI are large, with values of 0.017 and 0.012 Å for the two states, and this parallels the results obtained for the singlet excited states.[11] It seems that the states with geometric constrains imply more difference between PBE0 and SAC-CI than other states.

Geometry optimization was also carried out for the $1^3A'$ and $1^3A''$ states of adenine, again restricting the system to C_s symmetry. These structures are saddle points because of the presence of the amino group (SI). The experimentally determined energy[64] (2.99 eV) was well reproduced for the $1^3A'$ state, with a computed value of 2.92 eV (SAC-CI). In this state, the geometrical changes compared to the ground state were calculated to be distributed over the whole molecule (Figure 3). Compared with the corresponding singlet state, the agreement between the geometrical parameters calculated by SAC-CI and TD-PBE0 for the triplet state was improved (Figure 3) and the rmsd values obtained by comparing the two methods are 0.009 and 0.010 Å for $1^3A'$ and $1^3A''$, respectively.

The computed SAC-CI and TD-PBE0 geometrical changes between the ground state and the lowest triplet state of 9,10-anthraquinone, coumarin, and 1,8-naphthalimide are compared in Figure 4, and the vertical transition energies and experimental values are summarized in Table 4 (see SI for details).[49,65,66] Frequency analysis performed at the stationary points showed that among the excited states examined (see section 3.1), several are local minima: three [1^3B_{3g}, 1^3A_u, and $1^3A'$(Cs)] for 9,10-anthraquinone, two ($1^3A'$ and $2^3A'$) for coumarin, and three (1^3A_1, 2^3A_1, and 1^3B_2) for 1,8-naphthalimide. To date, the geometries of the triplet excited states of 9,10-anthraquinone and 1,8-naphthalimide have not been theoretically studied by TD-DFT or ab initio calculations.

The equilibrium structures of the low-lying excited states of 9,10-anthraquinone, that is, 1^3B_{1g} and 1^3B_{1u}, were calculated by SAC-CI and TD-PBE0. In addition, structures of both 1^3B_{3g} and $1^3A'$ states were obtained by SAC-CI (see the SI). A sharp peak assigned to the 1^3B_{1g} state was measured at 2.53 eV[49] and the calculated energy is on the spot (2.51 eV with SAC-CI). Based on the geometrical changes in the 1^3B_{1g} and 1^3B_{1u} states (significant variations of the $O_1{-}C_2$ and $C_2{-}C_3$ bond lengths),

dx.doi.org/10.1021/ct5003797 | J. Chem. Theory Comput. 2014, 10, 3969−3979

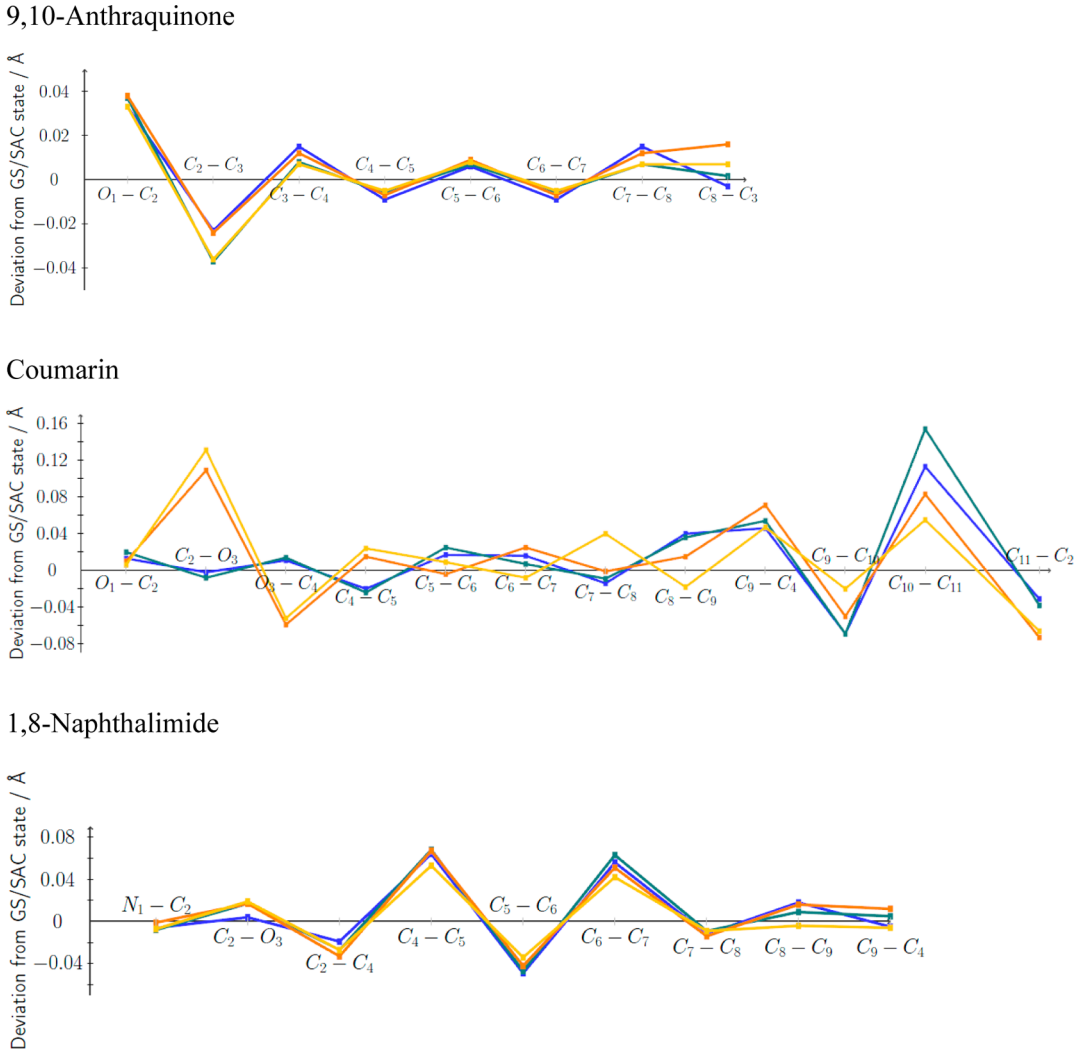

Figure 4. Geometry changes relative to the ground state for the singlet[11] and triplet excited states of 9,10-anthraquinone ($^{1,3}A'$), coumarin ($^{1,3}A'$), and 1,8-naphthalimide ($^{1,3}A_1$) calculated by SAC-CI (singlet, orange; triplet, blue) and TD-PBE0 (singlet, yellow; triplet, green).

we can state that the excitation is localized in the central moiety for these states. On the contrary, the structural changes for the $1^3A'$ state are not so remarkable and the excitation is rather delocalized. These findings are consistent with the transition character as well as with the topology of relevant molecular orbitals involved in the excitation. The rmsd values for the bond lengths calculated with SAC-CI and TD-PBE0 are 0.010 and 0.018 Å for 1^3B_{1g} and 1^3B_{1u}, respectively. The deviations in phosphorescence energy between the two methods are small for the 1^3B_{1g} state, but very large for the 1^3B_{1u} state.

For coumarin, the lowest two states, $1^3A'$ and $2^3A'$, were considered and they have been confirmed to be local minima. Previously, the 0−0 phosphorescence of coumarin derivatives was evaluated at the PBE0/6-31+G(d) level and the results showed good agreement with the experimentally determined low-temperature spectra.[67] Here, the vertical emission was considered and the energies computed at the SAC-CI level, 2.26 and 2.92 eV, could be compared to the strong peak of the phosphorescence spectrum at ∼2.48 eV.[65] The excitation of the $1^3A'$ state is relatively localized to the C_9−C_{10}−C_{11} section of the molecule, and reversal of the single/double bond character occurs in that region. In contrast, the variation of the C_2−O_3 bond length is significant in the corresponding singlet state. As seen in Figure 4, the TD-PBE0 and SAC-CI calculations gave the same trends for the bond-length changes, although the geometry changes are sometimes more pronounced with the former approach.

For 1,8-naphthalimide, the equilibrium structures of the 1^3A_1, 1^3B_1, and 1^3B_2 states were obtained as local minima. The rmsd obtained when comparing SAC-CI and PBE0 are small for the two first states (0.006 Å) but much larger for the 1^3B_2 state, and the same holds for the deviation of phosphorescence energies that reach ca. 0.3 eV for the first two states but 0.5 eV for the latter. The emission energy for the first triplet state was computed to be 1.83 eV with SAC-CI, which for once, is not very close to the experimental reference (2.30 eV).[66] The bond length changes in C_4−C_5, C_5−C_6, and C_6−C_7 are large in the 1^3A_1 state, whereas the structural relaxation of 1^3B_1 state is centered on C_2−O_3, C_2−C_4, and C_4−C_5: the excitation is localized in different regions of the molecule for these two excited states.

Table 5 lists the calculated Stokes shifts, the differences between vertical absorption and emission energies, for all molecules. Because Stokes shifts are relative values that are derived from transition energies from different geometries, computational errors that are intrinsic to a specific approx-

dx.doi.org/10.1021/ct5003797 | J. Chem. Theory Comput. 2014, 10, 3969−3979

Table 4. Vertical Transition Energies from Phosphorescent States (ΔE, eV) and the RMSD Values of the Bond Lengths Calculated by TD-PBE0 and SAC-CI Optimization (Å)

molecule	state	ΔE (eV) TD-PBE0	ΔE (eV) SAC-CI	ΔE (eV) expt.	rmsd (Å)
furan	1^3B_2	2.09	2.97		0.014
	1^3A_1	4.51	4.93		0.008
pyrrole	1^3B_2	2.80	3.40		0.009
	1^3A_1	4.69	5.04		0.003
pyridine	1^3A_1	2.73	3.32		0.009
	1^3B_1	3.21	3.59		0.005
	1^3B_2	4.18	4.54		0.003
p-benzoquinone	1^3A_u	1.61	2.29	2.25,[a] 2.28[b]	0.009
	1^3B_{1g}	1.73	2.41	2.30,[a] 2.31[b]	0.008
uracil	$1^3A'$	1.88	2.70		0.017
	$1^3A''$	3.14	3.41		0.012
adenine	$1^3A'$	2.41	2.92	2.99[c]	0.009
	$1^3A''$	3.56	3.74		0.010
9,10-anthraquinone	1^3B_{1g}	2.28	2.51	~2.53[d]	0.010
	1^3B_{1u}	1.80	2.91		0.018
coumarin	$1^3A'$	1.54	2.26	~2.48[e]	0.013
	$2^3A'$	2.53	2.93		0.029
1,8-naphthalimide	1^3A_1	1.52	1.83	2.31[f]	0.006
	1^3B_1	2.91	3.25		0.006
	1^3B_2	3.08	3.58		0.021

[a]Ref 49. [b]Ref 63. [c]Ref 64. [d]Ref 49 (maximum peak ~490 nm). [e]Ref 65 (maximum second peak ~500 nm). [f]Ref 66.

imation and not significantly dependent on molecular geometry would be canceled. As a result, these values are useful for comparing the calculated transition energies and optimized geometries obtained by different methodologies: differences in the Stokes shifts calculated by the TD-PBE0 and SAC-CI methods straightforwardly reflect differences in the optimized geometries and electronic structures in the excited states.[68] The correlation between the Stokes shifts calculated for both methods is shown in Figure 5. The values calculated by TD-PBE0 and SAC-CI present good agreement for many excited states, with a difference of 0.1 eV or less. Significantly larger deviations were found for the 1^3B_2 state of furan, the $1^3A'$ state of uracil, the 1^3B_{1u} state of 9,10-anthraquinone and the $1^3A'$ state of coumarin (see Figure 5). These large deviations can be attributed to differences between the optimized geometries. In these four states, the TD-PBE0/SAC-CI rmsd values computed for the optimized bond lengths are indeed larger than 0.01 Å, and the maximum deviations regarding absolute bond lengths are also large: (i) in the 1^3B_2 state of furan, the difference in the optimized C_2-C_3 bond length calculated by the two methods is 0.02 Å; (ii) in the $1^3A'$ state of uracil, the largest deviation of 0.042 Å is found for the C_7-C_8 bond; (iii) in the 1^3B_{1u} state of 9,10-anthraquinone, the C_2-C_3 bond length optimized by SAC-CI is 0.025 Å longer than that obtained at the TD-PBE0 level; (iv) in the $1^3A'$ state of coumarin, the $C_{10}-C_{11}$ bond

Table 5. Stokes Shifts (eV) Calculated at the TD-PBE0 and SAC-CI Levels with the D95(d) Basis Set and the Difference between the Values

molecule	state	TD-PBE0	SAC-CI	difference
furan	1^3B_2	1.57	1.19	0.38
	1^3A_1	0.62	0.52	0.10
pyrrole	1^3B_2	1.19	1.03	0.16
	1^3A_1	0.52	0.45	0.07
pyridine	1^3A_1	0.95	0.78	0.17
	1^3B_1	1.20	0.91	0.29
	1^3B_2	0.33	0.32	0.01
p-benzoquinone	1^3A_u	0.27	0.17	0.10
	1^3B_{1g}	0.60	0.46	0.14
uracil	$1^3A'$	1.49	0.97	0.52
	$1^3A''$	1.22	1.18	0.04
adenine	$1^3A'$	1.10	0.89	0.21
	$1^3A''$	1.24	1.10	0.14
9,10-anthraquinone	1^3B_{1g}	0.29	0.23	0.06
	1^3B_{1u}	0.99	0.57	0.42
coumarin	$1^3A'$	1.19	0.83	0.36
	$2^3A'$	1.05	1.07	−0.02
1,8-naphthalimide	1^3A_1	0.76	0.77	−0.01
	1^3B_1	0.68	0.58	0.10
	1^3B_2	0.34	0.41	−0.07

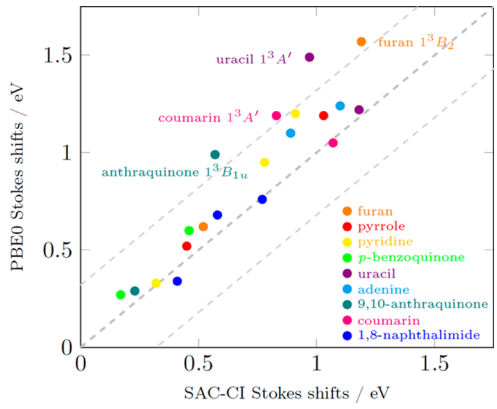

Figure 5. Comparison between the Stokes shifts calculated at the TD-PBE0 and SAC-CI levels.

length optimized by the SAC-CI method is 0.04 Å shorter than its TD-PBE0 counterpart. These differences in optimized bond lengths are remarkably large in comparison with other bonds (see the SI) and large rmsd values are also obtained in the $2^3A'$ state of coumarin and the 1^3B_2 state of 1,8-naphtalimide. For the latter states, however, the Stokes shifts calculated at the TD-PBE0 and SAC-CI levels were in good agreement, which indicates that some errors were canceled out in these states.

In short, we could state that TD-PBE0 generally provides geometrical variations between ground and triplet states that are similar to those computed with SAC-CI, indicating that TD-DFT can be used to determine structures and the same holds

dx.doi.org/10.1021/ct5003797 | J. Chem. Theory Comput. 2014, 10, 3969−3979

for Stokes shifts. For absolute phosphorescence energies, however, TD-PBE0 tends to yield small values and this can be mainly related to a "vertical" error than a "structural" discrepancy.

3.3. Effect of the Exchange-Correlation Functional. To estimate the effect of the exchange-correlation functional, the emission energies and structural features were calculated by using M06,[69] M06-2X,[70] B3LYP,[13] CAM-B3LYP,[71] and ωB97X-D,[72] and the results were compared with those obtained by using SAC-CI (Figure 6). Regarding the structural features, total rmsd values were calculated by comparing bond lengths, bond angles, and dihedral angles of all the studied molecules calculated by SAC-CI and by each of the functionals. The total rmsd value calculated with the CAM-B3LYP functional is not reported here because several optimizations did not converge with this functional. Among the five other functionals, PBE0 gave the most accurate results, with a global rmsd of ca. 0.012 Å. M06 provided a rmsd of 0.013 Å, whereas the remaining functionals gave rmsd values larger than 0.015 Å. Generally, all functionals showed similar behavior for the same electronic state. For example, for the $^3B_2$ state of pyrrole, the calculated rmsd varied from 0.005 Å (M06) to 0.008 Å (B3LYP), with an average value of 0.007 Å. We note that molecules of small size, i.e., furan, pyrrole, pyridine, and *p*-benzoquinone, in general present smaller rmsd values than larger systems. The range-separated hybrids become better for larger system, which is consistent with the previous results for the vertical transitions.[7] The rmsd values computed for adenine, 1,8-naphthalimide, 9,10-anthraquinone, coumarin, and uracil are all larger than 0.01 Å. Although PBE0 does not always provide the best results when each state is analyzed separately, this functional provides coherent results for all the computed electronic states. This justifies the use of this functional in the former sections.

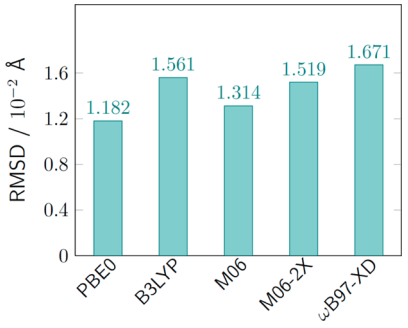

Figure 6. Total rmsd values calculated for selected vertical emitting states, using various functionals.

The energies of the vertical splitting between the singlet and triplet excited states have also been computed by using the same functionals, with the exception of CAM-B3LYP. With respect to the triplet state energies, as opposed to singlet state energies, M06-2X clearly presents the best performance of all the tested functionals. For each functional, the difference between the results obtained by SAC-CI and TD-DFT did not exceed 1.11 eV for the $^3B_{1g}$ state of 9,10-anthraquinone and, for some states, this deviation became notably small. For example, the $^3A''$ state of uracil showed deviations that ranged from 0.44 eV for B3LYP to 0.15 eV for ωB97X-D, and the same behavior was found for various other states. Indeed, 11 out of the 20 states examined present deviations of less than 0.55 eV for each functional: the $^3A_1$ state of furan, the $^3B_1$ state of pyrrole, the $^3B_1$ and $^3B_2$ states of pyridine, the $^3A''$ state of uracil and adenine, the $^3B_{1u}$ state of 9,10-anthraquinone, the $^3A'$ state of coumarin, and all computed states of 1,8-naphthalimide.

4. SUMMARY

We have performed direct SAC-CI and TD-PBE0 benchmark calculations for the geometries, electronic properties, and phosphorescence energies of a large panel of triplet excited states. The low-lying $\pi\pi^*$ and $n\pi^*$ triplet states of nine heterocyclic compounds, furan, pyrrole, pyridine, *p*-benzoquinone, uracil, adenine, 9,10-anthraquinone, coumarin, and 1,8-naphthalimide, as well as Rydberg states were solved, some of which have been investigated for the first time. The benchmark calculations of SAC-CI and TD-PBE0 demonstrated that these two methods provide consistent descriptions of the triplet excited-state geometries of these heterocyclic compounds, with relatively small deviations. TD-PBE0 is also able to reproduce the ordering of the excited-states for most cases, but, in general, it provides too small transition energies from and to the triplet state, an error that can be partly fixed using M06-2X. Despite the underestimation of the phosphorescence energies, the Stokes shifts calculated by these methods, which reflect geometry changes with high sensitivity, agree well. The deviations between the methods are enhanced in the vertical transition from the triplet equilibrium structure.

■ ASSOCIATED CONTENT

Supporting Information

Detailed SAC/SAC-CI results with Cartesian coordinates, CIS vibrational analysis, and detailed TD-DFT results with various basis sets and functionals. This material is available free of charge via the Internet at http://pubs.acs.org.

■ AUTHOR INFORMATION

Corresponding Authors

*Email: ehara@ims.ac.jp.

*Email: carlo-adamo@chimie-paristech.fr.

Notes

The authors declare no competing financial interest.

■ ACKNOWLEDGMENTS

M.E. and R.F. acknowledge a Grant-in-Aid for Scientific Research from the Japanese Society for the Promotion of Science (JSPS). The work was also supported by Nanotechnology Platform Program (Molecule and Material Synthesis) of the Ministry of Education, Culture, Sports, Science, and Technology (MEXT) of Japan. The SAC-CI calculations were partly performed using the Research Center for Computational Science in Okazaki, Japan. D.J. acknowledges the European Research Council (ERC) and the Région des Pays de la Loire for financial support in the framework of a Starting Grant (Marches 278845) and a *recrutement sur poste stratégique*, respectively.

■ REFERENCES

(1) Baldo, M. A.; O'Brien, D. F.; Thompson, M. E.; Forrest, S. R. *Phys. Rev. B* **1999**, *60*, 14422−14428.
(2) Evans, R. C.; Douglas, P.; Winscom, C. J. *Coord. Chem. Rev.* **2006**, *250*, 2093−2126.
(3) Singh-Rachford, T. N.; Castellano, F. N. *Coord. Chem. Rev.* **2010**, *254*, 2560−2573.
(4) Smith, M. B.; Michl, J. *Chem. Rev.* **2010**, *110*, 6891−6936.

(5) Silva-Junior, M. R.; Schreiber, M.; Sauer, S. P. A.; Thiel, W. *J. Chem. Phys.* **2008**, *129*, 104103.
(6) Silva-Junior, M. R.; Schreiber, M.; Sauer, S. P. A.; Thiel, W. *J. Chem. Phys.* **2010**, *133*, 174318.
(7) Jacquemin, D.; Wathelet, V.; Perpète, E. A.; Adamo, C. *J. Chem. Theory Comput.* **2009**, *5*, 2420−2435.
(8) Jacquemin, D.; Perpète, E. A.; Ciofini, I.; Adamo, C.; Valero, R.; Zhao, Y.; Truhlar, D. G. *J. Chem. Theory Comput.* **2010**, *6*, 2071−2085.
(9) Jacquemin, D.; Perpete, E. A.; Ciofini, I.; Adamo, C. *J. Chem. Theory Comput.* **2010**, *6*, 1532−1537.
(10) Guido, C. A.; Jacquemin, D.; Adamo, C.; Mennucci, B. *J. Phys. Chem. A* **2010**, *114*, 13402−13410.
(11) Bousquet, D.; Fukuda, R.; Maitarad, P.; Jacquemin, D.; Ciofini, I.; Adamo, C.; Ehara, M. *J. Chem. Theory Comput.* **2013**, *9*, 2368−2379.
(12) Guido, C. A.; Stefan, K.; Kongsted, J.; Mennucci, B. *J. Chem. Theory Comput.* **2013**, *9*, 2209−2220.
(13) Becke, A. D. *J. Chem. Phys.* **1993**, *98*, 5648−5652.
(14) Adamo, C.; Barone, V. *J. Chem. Phys.* **1998**, *108*, 664−675.
(15) Nakatsuji, H. *Chem. Phys. Lett.* **1978**, *59*, 362−364.
(16) Nakatsuji, H. *Chem. Phys. Lett.* **1979**, *67*, 329−333.
(17) Mukherjee, D.; Mukherjee, P. K. *Chem. Phys.* **1979**, *39*, 325−335.
(18) Koch, H.; Jorgensen, P. *J. Chem. Phys.* **1990**, *93*, 3333−3344.
(19) Geertsen, J.; Rittby, M.; Bartlett, R. J. *Chem. Phys. Lett.* **1989**, *164*, 57−62.
(20) Stanton, J. F.; Bartlett, R. J. *J. Chem. Phys.* **1993**, *98*, 7029−7039.
(21) Nakatsuji, H. *Acta Chim. Hung.* **1992**, *129*, 719−776.
(22) Ehara, M.; Hasegawa, J.; Nakatsuji, H. SAC-CI Method Applied to Molecular Spectroscopy. In *Theory and Applications of Computational Chemistry: The First 40 Years, A Vol. of Technical and Historical Perspectives*; Dykstra, C. E., Frenking, G., Kim, K. S., Scuseria, G. E., Eds.; Elsevier: Oxford, 2005; pp 1099−1141.
(23) Nakajima, T.; Nakatsuji, H. *Chem. Phys. Lett.* **1997**, *280*, 79−84.
(24) Nakajima, T.; Nakatsuji, H. *Chem. Phys.* **1999**, *242*, 177−193.
(25) Ishida, M.; Toyota, K.; Ehara, M.; Nakatsuji, H.; Frisch, M. J. *J. Chem. Phys.* **2004**, *120*, 2593−2605.
(26) Ishida, M.; Toyota, K.; Ehara, M.; Nakatsuji, H. *Chem. Phys. Lett.* **2001**, *350*, 351−358.
(27) Ehara, M.; Oyagi, F.; Abe, Y.; Fukuda, R.; Nakatsuji, H. *J. Chem. Phys.* **2011**, *135*, 044316.
(28) Fukuda, R.; Nakatsuji, H. *J. Chem. Phys.* **2008**, *128*, 094105.
(29) Tozer, D. J.; Handy, N. C. *Phys. Chem. Chem. Phys.* **2000**, *2*, 2117−2121.
(30) Santoro, F.; Improta, R.; Lami, A.; Bloino, J.; Barone, V. *J. Chem. Phys.* **2007**, *126*, 184102.
(31) Quartarolo, A. D.; Sicilia, E.; Russo, N. *J. Chem. Theory Comput.* **2009**, *5*, 1849−1857.
(32) Peach, M. J. G.; Tozer, D. J. *J. Phys. Chem. A* **2012**, *116*, 9783−9789.
(33) Sears, J. S.; Koerzdoerfer, T.; Zhang, C.-R.; Brédas, J.-L. *J. Chem. Phys.* **2011**, *135*, 151103.
(34) Frisch, M. J.; Trucks, G. W.; Schlegel, H. B.; Scuseria, G. E.; Robb, M. A.; Cheeseman, J. R.; Scalmani, G.; Barone, V.; Mennucci, B.; Petersson, G. A.; Nakatsuji, H.; Caricato, M.; Li, X.; Hratchian, H. P.; Izmaylov, A. F.; Bloino, J.; Zheng, G.; Sonnenberg, J. L.; Hada, M.; Ehara, M.; Toyota, K.; Fukuda, R.; Hasegawa, J.; Ishida, M.; Nakajima, T.; Honda, Y.; Kitao, O.; Nakai, H.; Vreven, T.; Montgomery, Jr., J. A.; Peralta, J. E.; Ogliaro, F.; Bearpark, M.; Heyd, J. J.; Brothers, E.; Kudin, K. N.; Staroverov, V. N.; Kobayashi, R.; Normand, J.; Raghavachari, K.; Rendell, A.; Burant, J. C.; Iyengar, S. S.; Tomasi, J.; Cossi, M.; Rega, N.; Millam, J. M.; Klene, M.; Knox, J. E.; Cross, J. B.; Bakken, V.; Adamo, C.; Jaramillo, J.; Gomperts, R.; Stratmann, R. E.; Yazyev, O.; Austin, A. J.; Cammi, R.; Pomelli, C.; Ochterski, J. W.; Martin, R. L.; Morokuma, K.; Zakrzewski, V. G.; Voth, G. A.; Salvador, P.; Dannenberg, J. J.; Dapprich, S.; Daniels, A. D.; Farkas, Ö.; Foresman, J. B.; Ortiz, J. V.; Cioslowski, J.; Fox, D. J. *Gaussian 09, Revision B.01*; Gaussian, Inc.: Wallingford, CT, 2010.
(35) Dunning, T. H., Jr. *J. Chem. Phys.* **1970**, *53*, 2823−2833.
(36) Krishnan, R.; Binkley, J. S.; Seeger, R.; Pople, J. A. *J. Chem. Phys.* **1980**, *72*, 650−654.
(37) Dunning, T. H., Jr. *J. Chem. Phys.* **1989**, *90*, 1007−1023.
(38) Dunning, T. H., Jr.; Harrison, P. J. In *Mordern Theoretical Chemistry*; Schaefer, H. F., III., Ed.; Plenum Press: New York, 1977; Vol. *2*; pp 1−28.
(39) Nakatsuji, H. *Chem. Phys.* **1983**, *75*, 425−441.
(40) Toyota, K.; Ishida, M.; Ehara, M.; Frisch, M. J.; Nakatsuji, H. *Chem. Phys. Lett.* **2003**, *367*, 730−736.
(41) Flicker, M. W.; Moser, O. A.; Kupperman, A. *J. Chem. Phys.* **1976**, *64*, 1315−1321.
(42) Walker, I. C.; Palmer, M. H.; Hopkirk, A. *Chem. Phys.* **1990**, *141*, 365−378.
(43) van Veen, E. H.; Plantenga, F. L. *Chem. Phys. Lett.* **1975**, *80*, 28−31.
(44) Doering, J. P.; Moore, J. H., Jr. *J. Chem. Phys.* **1972**, *56*, 2176−2178.
(45) Wan, J.; Meller, J.; Hada, M.; Ehara, M.; Nakatsuji, H. *J. Chem. Phys.* **2000**, *113*, 7853−7866.
(46) Lorentzon, J.; Fulscher, M. P.; Roos, B. O. *Theor. Chim. Acta* **1995**, *92*, 67−81.
(47) Bolovinos, A.; Tsekeri, P.; Philis, J.; Pantos, E.; Andrisopoulus, G. *J. Mol. Spectrosc.* **1984**, *103*, 240−256.
(48) Wan, J.; Hada, M.; Ehara, M.; Nakatsuji, H. *J. Chem. Phys.* **2001**, *114*, 5117−5123.
(49) Itoh, T. *Chem. Rev.* **1995**, *95*, 2351−2368.
(50) Trommsdorff, H. P. *J. Chem. Phys.* **1972**, *56*, 5358−5372.
(51) Koyanagi, M.; Kogo, Y.; Kanda, Y. *J. Mol. Spectrosc.* **1970**, *34*, 450.
(52) Koyanagi, M.; Kogo, Y.; Kanda, Y. *Mol. Phys.* **1971**, *20*, 747.
(53) Abouaf, R.; Pommier, J.; Dunet, H. *Chem. Phys. Lett.* **2003**, *381*, 486−494.
(54) Nguyen, M. T.; Zhang, R.; Nam, P.-C.; Ceulemans, A. *J. Phys. Chem. A* **2004**, *108*, 6554−6561.
(55) Pou-Amerigo, R.; Merchan, M.; Orti, E. *J. Chem. Phys.* **1999**, *110*, 9536−9546.
(56) Climent, T.; Gonzalez-Luque, R.; Merchan, M.; Serrano-Andres, L. *Chem. Phys. Lett.* **2007**, *441*, 327−331.
(57) Honda, Y.; Hada, M.; Ehara, M.; Nakatsuji, H. *J. Phys. Chem. A* **2002**, *106*, 3838−3849.
(58) Epifanovsky, E.; Kowalski, K.; Fan, P.-D.; Valiev, M.; Matsika, S.; Krylov, A. I. *J. Phys. Chem. A* **2008**, *112*, 9983−9992.
(59) Harrigan, E. T.; Chakrabarti, A.; Hirota, N. *J. Am. Chem. Soc.* **1976**, *98*, 3460−3465.
(60) Gromov, E. V.; Trofimov, A. B.; Vikovskaya, N. M.; Schirmer, J.; Köppel, H. *J. Chem. Phys.* **2003**, *119*, 737−753.
(61) Celani, P.; Werner, H.-J. *J. Chem. Phys.* **2003**, *119*, 5044−5057.
(62) Cai, Z.-L.; Reimers, J. R. *J. Phys. Chem. A* **2000**, *104*, 8389−8408.
(63) Itoh, T.; Hashimoto, R. *J. Lumin.* **2012**, *132*, 236−239.
(64) Polewski, K.; Zinger, D.; Trunk, J.; Sutherland, J. C. *Radiat. Phys. Chem.* **2011**, *80*, 1092−1098.
(65) Mantulin, W. W.; Song, P. S. *J. Am. Chem. Soc.* **1973**, *95*, 5122−5129.
(66) Manna, A.; Chakravorti, S. *Photochem. Photobiol.* **2010**, *86*, 47−54.
(67) Jacquemin, D.; Perpète, E. A.; Scalmani, G.; Frisch, M. J.; Assfeld, X.; Ciofini, I.; Adamo, C. *J. Chem. Phys.* **2006**, *125*, 164324.
(68) Fukuda, R.; Ehara, M. *Phys. Chem. Chem. Phys.* **2014**, *15*, 17426−17434.
(69) Zhao, Y.; Truhlar, D. G. *Theor. Chem. Acc.* **2008**, *120*, 215−241.
(70) Zhao, Y.; Truhlar, D. G. *J. Phys. Chem. A* **2006**, *110*, 5121−5129.
(71) Yanai, T.; Tew, D. P.; Handy, N. C. *Chem. Phys. Lett.* **2004**, *91*, 51−57.
(72) Chai, J. D.; Head-Gordon, M. *Phys. Chem. Chem. Phys.* **2008**, *10*, 6615−6620.